Mechanism of Morphology Development in Dynamically Cured EPDM/PP TPEs. I. Effects of State of Cure

F. GOHARPEY, A. A. KATBAB, H. NAZOCKDAST

Polymer Engineering Department, Amirkabir University, Tehran, Iran

Received 25 February 2000; accepted 3 July 2000

ABSTRACT: Attempts were made to follow and correlate morphological development with the crosslinking density, or state of cure (SOC), and the surface tension (γ) of the rubber phase in dynamically cured thermoplastic elastomers (TPEs) based on ethylene propylene diene rubber and polypropylene (PP) with 60/40 (w/w) ratios. Samples were taken from a hot running mixer without interruption and quickly quenched in liquid nitrogen both before and after the onset of vulcanization at various SOCs to carry out this process. The quick cooling of the samples prevented the coalescence and agglomeration of the dispersed rubber particles. A two-phase morphology with the rubber particles dispersed throughout the PP matrix was observed for the uncured but frozen samples, whereas unfrozen blend samples showed a particulate cocontinuous morphology in the uncured state. An increase in the mixing torque with the SOC was observed after the addition of a curing system. This was understood to be caused by the increase in the rubber crosslinking density and also by the enhancement of the interfacial adhesion between the cured rubber phase and the PP matrix, leading to the better wetting of the two phases. Above a certain crosslinking density (SOC), γ of the rubber particles decreased through elastic shrinkage. This phenomenon, together with the breakdown of the agglomerate structure formed by the cured rubber particles, led to a decrease in the mixing torque after a maximum was passed and, finally, to a defined morphology. Based on the obtained results, a four-stage model is proposed to describe the microstructural development in dynamically vulcanized TPEs. Dynamic mechanical thermal analysis and differential scanning calorimetry results are also used to support the model. © 2001 John Wiley & Sons, Inc. J Appl Polym Sci 81: 2531–2544, 2001

Key words: thermoplastic elastomer; dynamic cure; ethylene propylene diene rubber/polypropylene (EPDM/PP); morphology; state of cure; agglomeration; surface tension

INTRODUCTION

Dynamically vulcanized thermoplastic elastomer (TPE) blends were first presented by Fisher[1,2] and since then have been widely used in the rubber and plastic industries.[3,4] These materials can be melt-processed and shaped by conventional thermoplastic processing methods but, in their final state, show an elastic recovery similar to that of ordinary vulcanized rubbers.[5,6] The addition of a small quantity of a vulcanizing system during the melt-mixing of rubber and plastic leads to the *in situ* vulcanization of the dispersed rubber particles. The outstanding properties of these materials are mainly attributed to their specific microstructure, which consists of a continuous plastic matrix with tiny rubber particles dispersed throughout the matrix. This enables

Correspondence to: A. A. Katbab (katbab@cic.aku.ac.ir).

Journal of Applied Polymer Science, Vol. 81, 2531–2544 (2001)

Table I Characteristics of the Materials Used

Material		Characteristics
PP	MFI	6.0 g/10 min
	Density	0.91 g/cm^3
	T_m	165°C
EPDM	Mooney viscosity ML (1 + 4) 125°C	77
	Ethylene content	52%
	Termonomer content	4.5%
	Density	0.89 g/cm^3
	Curing rate	Fast

the blend to be melt-processed even though the rubber particles are crosslinked. Both the physical and rheological properties of these materials are, therefore, dependent on their morphology.[7–9] Much work has been done that deals with the mechanical and rheological properties of dynamically cured TPEs.[3,9–11] Also, a few studies have been carried out, mainly to characterize the microstructure of dynamically cured TPEs based on different rubber–plastic blend systems.[3,7,12–14] The development of morphology for dynamically vulcanized nitryl butadiene rubber/nylon (NBR/nylon) was also modeled by Bhowmick and Inoue[15] without consideration of the change in rubber surface tension (γ) with the time of mixing. However, effects of the change in γ of the rubber particles and interfacial adhesion between the two phases on the development of the blend morphology have not been deeply investigated. The goal of this work was to follow morphology change during the mixing process for an ethylene propylene diene rubber (EPDM)/polypropylene (PP) blend system (60/40 w/w) with a crosslinking agent. Correlations were done between the change in the rubber particles' surface energy, which was expected to vary with crosslinking density and state of cure (SOC). A scanning electron microscopy (SEM) examination was carried out on the quickly quenched uncured samples taken from the hot running mixer and also after the onset of the crosslinking of the rubber phase for the samples. After consideration of the variation of interfacial adhesion between the two phases during the mixing process, a four-stage model is suggested and discussed. Effects of curing parameters such as scorch time, curing rate, and EPDM structural parameters on morphology were also studied; this is presented in the second part of this series.

EXPERIMENTAL

Materials

The basic characteristics of the polymer used in this study are listed in Table I. Injection-grade PP from Himont Co. (Italy) and EPDM based on ENB as a diene monomer and supplied by Keltan from DSM Elastomers Europe (Holland) were used as commercially available.

Blends Preparation

The composition and recipes of the blend used in this work are given in Table II, where the letters *A* and *B* denote blends with and without crosslinking systems, respectively. We carried out the blending of the two polymers by first feeding the PP into a small-scale laboratory Haake internal mixer (Rheocord 90; Germany) at 180°C with a rotor speed of 60 rpm; this was followed by the addition of EPDM in the molten state of PP, and mixing was continued for 4 min. For the formulations with a crosslinking system, zinc oxide and stearic acid were added into the polymer mix, and mixing was continued for 1 min. Accelerators, including TMTD and MBTS, were charged, and after 30 s, sulfur was added. The onset of the vulcanization of the rubber phase was indicated by an increase in the mixing torque. At each desired mixing time, samples were taken from the mixer without the mixing process being stopped, both before and after the addition of curatives.

Morphology Studies

To follow the effects of coalescence on the morphology of the blend, we prepared two groups of samples for SEM examination. These included uncured samples, which were allowed to cool at room temperature after removal from the hot run-

Table II Recipes for the Preparation of Dynamically Cured EPDM/PP Blends (60/40 w/w)

Ingredient	A	B	C
EPDM	60	60	40
PP	40	40	60
ZnO	—	5	4.6
Stearic Acid	—	1.5	1.38
MBTS	—	1.5	1.38
TMTD	—	0.9	0.828
Sulfur	—	1.4	1.288

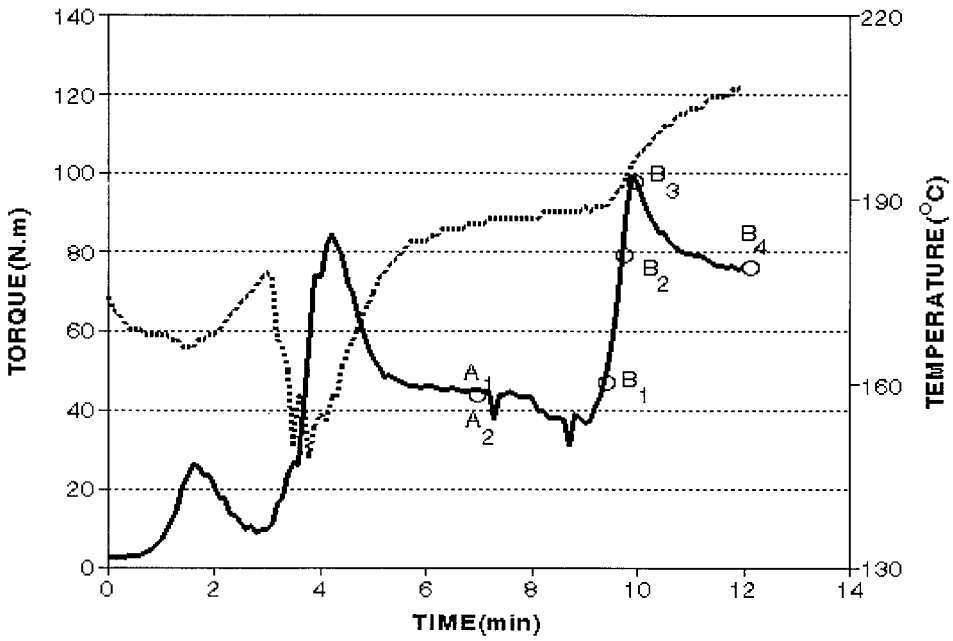

Figure 1 Variation of the torque (—) and temperature (· · ·) versus time at different mixing stages for the preparation of EPDM/PP (60/40 w/w) dynamically cured TPE.

ning mixer, and uncured samples that were frozen immediately after being taken from the hot mix. These are denoted A_1 and A_2, respectively. Samples that were taken from the hot running mix at different SOCs and cooled at room temperature are denoted B_1, B_2, B_3, and B_4.

To study the morphology of the blend samples, we stained cryogenically fractured surfaces with osmium tetroxide vapor for 4 h. The stained surfaces were then sputter-coated with gold and viewed with a scanning electron microscope (model XL 30) made by Phillips Co. (Holland).

Thermal Behavior Studies

For our purposes, a dynamic mechanical thermal analysis (DMTA) model PL (England) was used. The test was performed on the samples within the temperature range of −100°C to 100°C at a fixed frequency of 1 Hz and a heating rate of 3°C/min. Also, a differential scanning calorimeter (model STA-625) made by Rheometric Scientific Co. (England) was used to study the thermal characteristics and degree of crystallinity of the samples from the measured heat of fusion at a heating rate of 20°C/min.

Surface Energy Measurement

γ and its associated nonpolar (dispersion) and polar components (γ^d and γ^p, respectively) were evaluated for the samples in the form of film according to the Ownes–Wendt–Rabel and Kaelble method with a Kruss instrument (model G40; Germany).

In this method, the static contact angle between drops of four different liquids, such as water, ethylene glycol, formamid, and 1,5-pentanediol, is measured separately, and then the sample γ and its components are calculated and reported by the machine. The interfacial tension (γ_{12}) between the surfaces of PP and EPDM vulcanizate was obtained from the well-known harmonic mean equation (1).[16] Also, the work of adhesion (w_a) between the two phases was calculated by eq. (2) as follows:

$$\gamma_{12} = \gamma_1 + \gamma_2 - \frac{4\gamma_1^d\gamma_2^d}{\gamma_1^d + \gamma_2^d} - \frac{4\gamma_1^p\gamma_2^p}{\gamma_1^p + \gamma_2^p} \quad (1)$$

$$w_a = \gamma_1 + \gamma_2 - \gamma_{12} \quad (2)$$

where γ_1 and γ_2 denote the γ values of PP and EPDM, respectively.

RESULTS AND DISCUSSION

In Figure 1, a typical curve showing the variation of the mixing torque as a function of time related

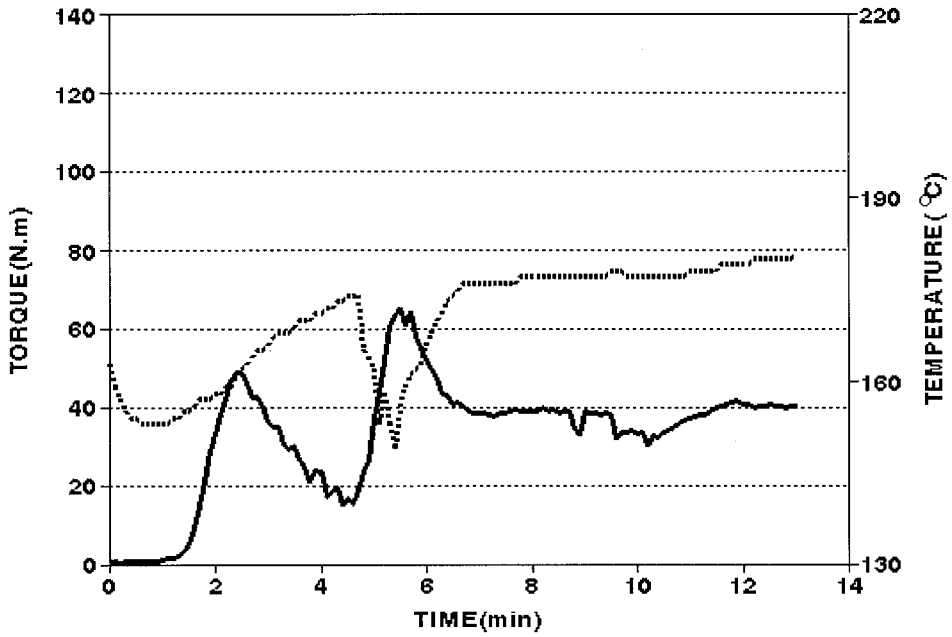

Figure 2 Variation of the torque (—) and temperature (· · ·) versus time at different mixing stages for the preparation of EPDM/PP (40/60 w/w) development in EPDM/PP (60/40 w/w) TPEs.

to the mixing stage of the EPDM/PP (60/40 w/w) blend system, composed of vulcanizing agents, is given. The first and second peak maxima correspond to the melting of PP and the feeding of the rubber into the mixer, respectively. The third peak is related to the stage of the dynamic vulcanization process. As the curing system was added, the mixing torque increased, and after passing through a maximum, it declined and then attained an almost constant value.

The increase in the mixing torque after the addition of vulcanizing agents could have been caused by both the increase in crosslinking density and γ of the rubber phase, which resulted in the enhancement of the interfacial adhesion with PP and, consequently, the better wetting of the two phases.[16] Moreover, as the vulcanization of the rubber droplets proceeded during mixing, the agglomerates of the rubber particles predominated compared with their coalescence as their viscous behavior was reduced. This could play a significant role in increasing the melt viscosity and, therefore, the mixing torque of the blend system during the dynamic vulcanization stage.

The formation of the agglomerate structure during vulcanization was shown by the lower torque observed for the blends with a rubber content of 40% (w/w; see Fig. 2), which is below the maximum packing volume (ϕ) of the rubber particles.[17]

In Table III, the effects of the vulcanization and SOC on γ and its associated components for

Table III Effects of the State of Cure on the EPDM Rubber ρ and Its Interfacial Adhesion with PP in the Solid State

Polymer	SOC (min)	γ (mN/m)	γ^d (mN/m)	γ^p (mN/m)	γ_{12} (mN/m)	w_a (mN/m)
PP		49.8	48.9	0.9		
EPDM	5	23.9	12.9	11.00	29.44	44.16
	6	25.6	20.6	5	14.3	61.1
	7	26.3	19.7	6.6	16.66	59.44
	11	23.8	17.4	6.4	19.128	54.472

EPDM was compounded with the sulfur curing system and compression molded at 175°C for various times.

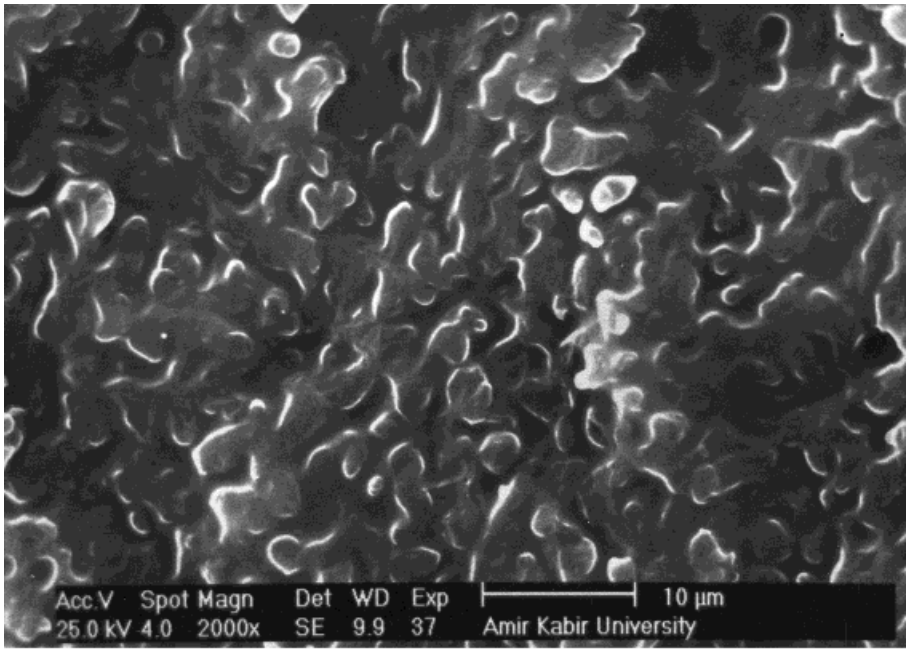

(A_1)

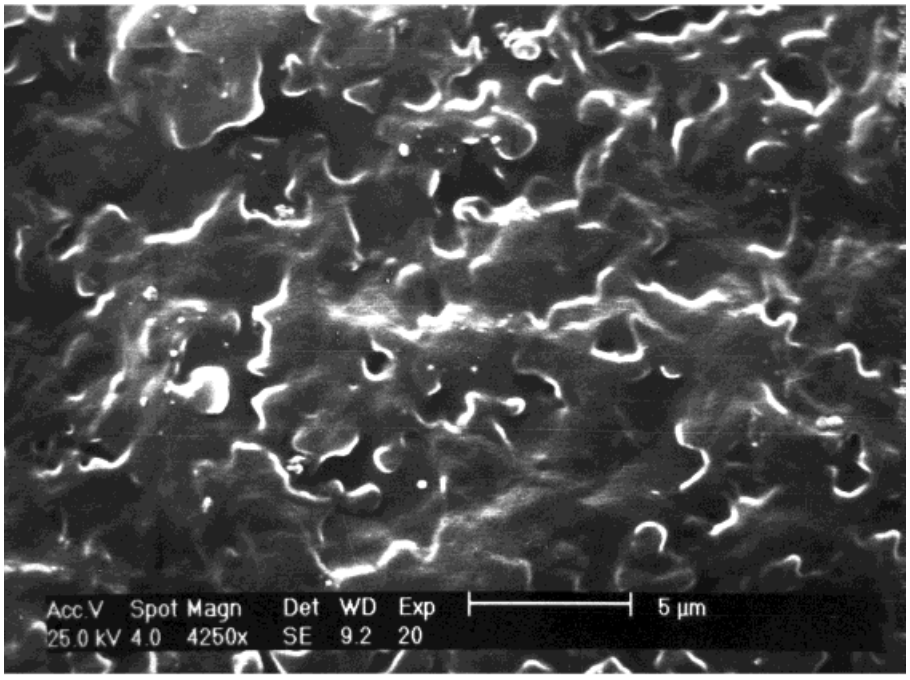

(A_2)

Figure 3 SEM photomicrographs of the uncured EPDM/PP (60/40 w/w) blend samples removed from the hot running mix: (A_1) frozen immediately after removal from the mix and (A_2) cooled at room temperature.

the EPDM rubber vulcanizate, together with the interfacial and w_a with PP in the solid state, are illustrated.

Measurements of γ of the polymers at the mixing temperature were not possible. Therefore, the data summarized in Table III were calculated at room temperature because γ of the polymers has been reported to vary linearly with temperature.[18–20]

It is clear that the interfacial adhesion between the PP and rubber vulcanizate increased with the

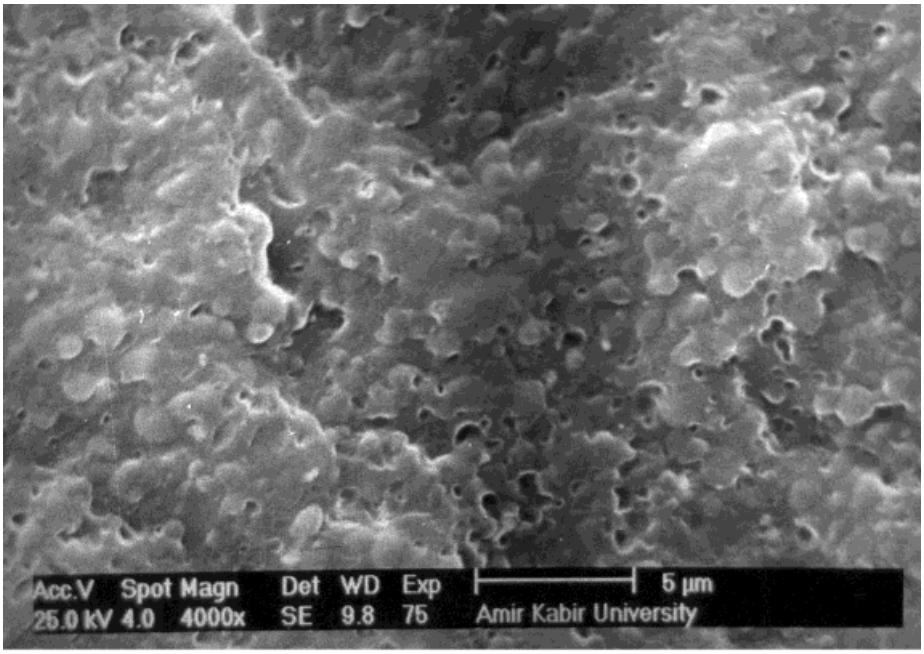

(B_1)

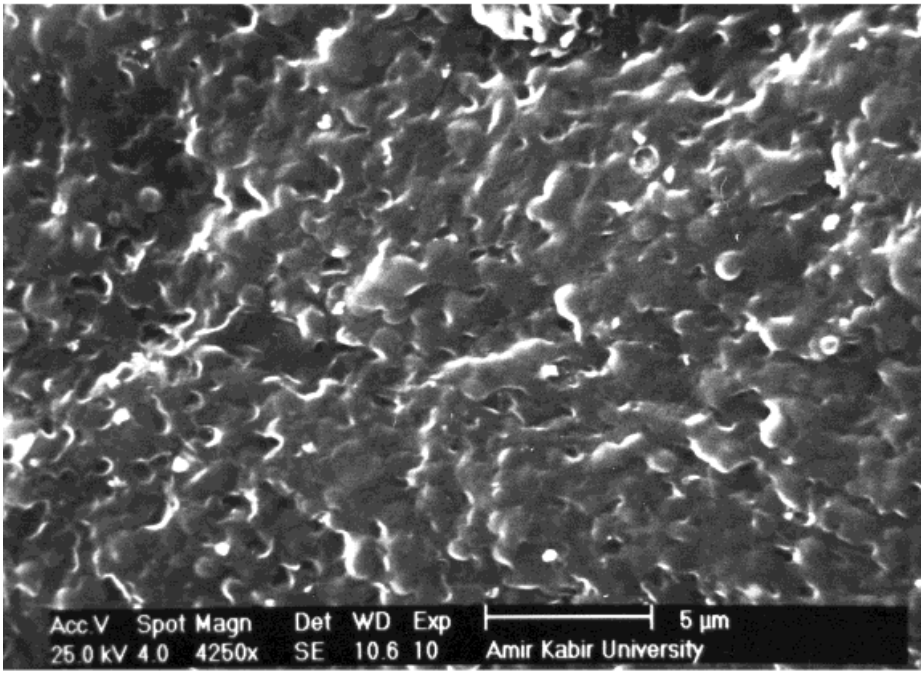

(B_2)

Figure 4 SEM photomicrographs of the EPDM/PP (60/40 w/w) blend samples dynamically crosslinked to different degrees: (B_1) removed at the early stage of vulcanization, (B_2) removed before reaching the torque maximum, (B_3) removed at the peak maximum of the torque, and (B_4) removed 2 min after the attainment of the torque maximum.

increase in the time of vulcanization (SOC). However, above a certain degree of crosslinking, the rubber γ showed slight decreases that could be the result of a reduction in the flexibility of both induced and permanent dipoles attached to the rubber segments within the vulcanized network

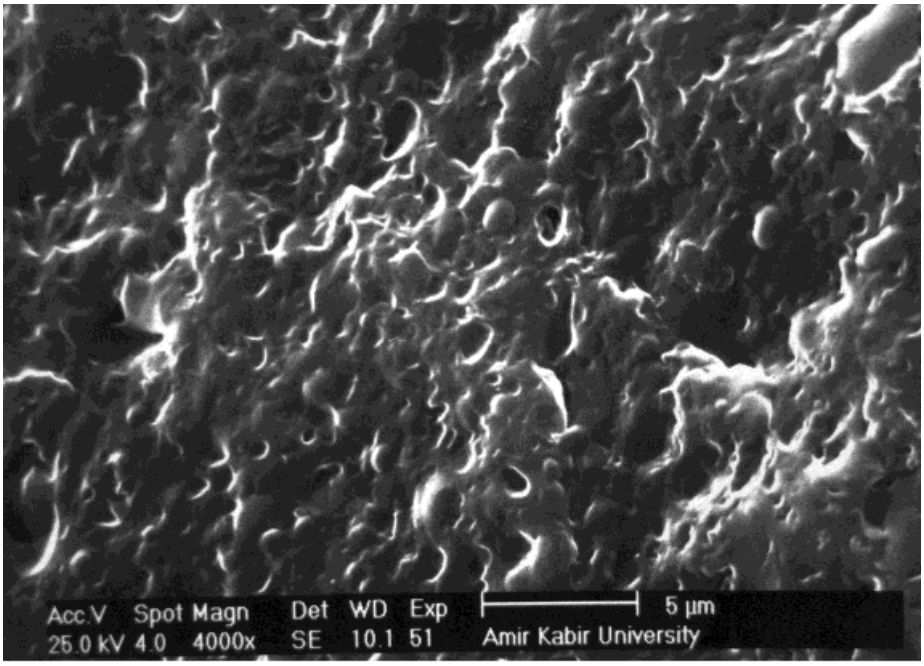

(B_3)

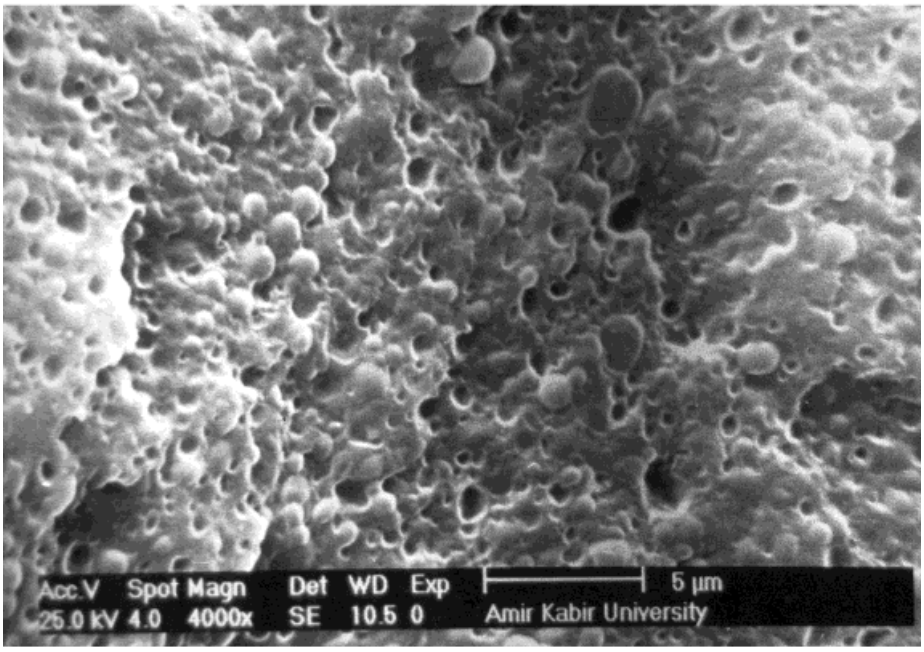

(B_4)

Figure 4 (*Continued from the previous page*)

and, therefore, a decrease in the total surface forces.[21] This was in accordance with the decrease in the rubber γ^p and the consequent weakening of interfacial adhesion (w_a) between the two phases.

The reduction in the mixing torque after the maximum (Fig. 1) could be partly caused by the tendency of the highly crosslinked rubber particles to minimize surface energy through elastic shrinkage, which helps the breakdown of the agglomerate structure formed during vulcanization. However, the breakdown of the agglomerate would lead to an increase in the interfacial adhe-

sion between the two phases as a result of an increase in the specific surface area of the rubber particles.

SEM photomicrographs for the uncured blend sample that was quickly frozen in liquid nitrogen after being removed from the mixer (A_1) and the sample that was cooled at room temperature (A_2) are given in Figure 3. It is obvious that the microstructure of the sample frozen in liquid nitrogen [Fig. 3(A_1)] exhibited a two-phase morphology consisting of rubber particles dispersed throughout the PP matrix, whereas a particulate cocontinuous morphology was obtained for the blend sample cooled at room temperature [Fig. 3(A_2)].

This led us to the conclusion that the coalescence of the uncured rubber droplets played an important role in controlling the morphology of the uncured blend samples.

Therefore, the morphology observed for the uncured blend sample cooled at room temperature is not necessarily similar to the morphology developed in the molten state during the mixing stage. The morphology of the EPDM/PP (60/40 w/w) dynamically cured blend samples taken from the mixer at different SOCs (B_1, B_2, B_3, and B_4) are illustrated in Figure 4. Dynamic vulcanization moved the blend microstructure from a melt–melt matrix dispersed for uncured samples into a well-defined particulate morphology consisting of cured rubber particles finely distributed throughout the PP matrix as the continuous phase.

Through a comparison of the SEM micrographs presented in Figure 5, we found that above a particular SOC, the agglomerate structure developed by the cured rubber particles during the crosslinking process [Fig. 5(A)] broke down into a more defined morphology [Fig. 5(B)]. The decrease in the mixing torque after the attainment of a maximum value could be considered a consequence of this phenomenon. For a better understanding of the microstructural development of the dynamically cured TPE samples, DMTA was performed on uncured and cured samples as presented in Figures 6–8.

It is evident from these figures that above the rubber glass-transition temperature, the storage moduli of both uncured but frozen and dynamically vulcanized blend samples were lower than those of uncured samples cooled at room temperature. Moreover, both dynamically cured and uncured but frozen blend samples exhibited higher damping characteristics compared with the uncured sample cooled at room temperature. The lower modulus and higher damping behavior of the first two samples could be attributed to less crystallinity and, therefore, more amorphous domains, compared with the uncured blend sample cooled at room temperature, as shown in Figures 9–11. The higher damping characteristics of the dynamically cured blend sample might also have been caused by the retarded response of the PP segments within the interface between the continuous matrix and the crosslinked rubber particles, on the one hand, and the inclusion of the PP segments into the rubber particles, on the other. The lower rate of increase in tan δ between 40 and 100°C for the uncured sample cooled at room temperature (Fig. 7) is thought to be caused by the higher crystallinity of the PP phase and, therefore, the lower contribution of the amorphous domains in the damping behavior of this sample.

To provide more information regarding the morphology development of the samples, we used composite models, such as the parallel model and Halpin Tsai equation.[22,23]

The parallel model corresponding to the maximum possible modulus and the Halpin Tsai equation are as follows:

$$M = M_1\phi_1 + M_2\phi_2 \tag{3}$$

$$\frac{M_1}{M} = (1 + A_1B_1\phi_2)/(1 - B_1\psi\phi_2) \tag{4}$$

$$B_i = \left(\frac{M_1}{M_2} - 1\right)/\left(\frac{M_1}{M_2} + A_i\right)$$

$$\psi = 1 + \frac{1 - \phi_m}{\phi_m^2}\,\phi_2$$

where M denotes the modulus of the composite and subscripts 1 and 2 refer to the PP and rubber phases, respectively. The constant A_i is defined by the morphology of the system and, for the elastomeric domains dispersed through a continuous hard matrix, has been reported to be 0.66[24]; ϕ_m is the maximum packing volume of the dispersed phase with a value of 0.64.[17] Figure 12 compares the experimental storage modulus data and the moduli predicted by these models.

Figure 12 shows that the values of the storage modulus for the uncured but frozen sample appear to be close to the upper bound of the Halpin Tsai equation. Although the storage modulus of the dynamically cured sample was higher than that of the frozen sample, it was still close to

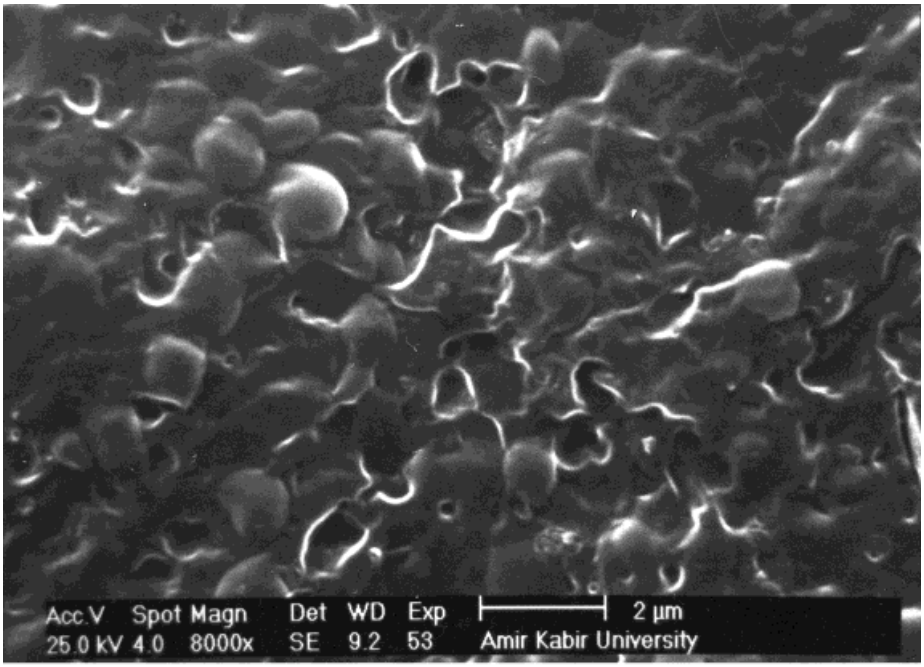

(A)

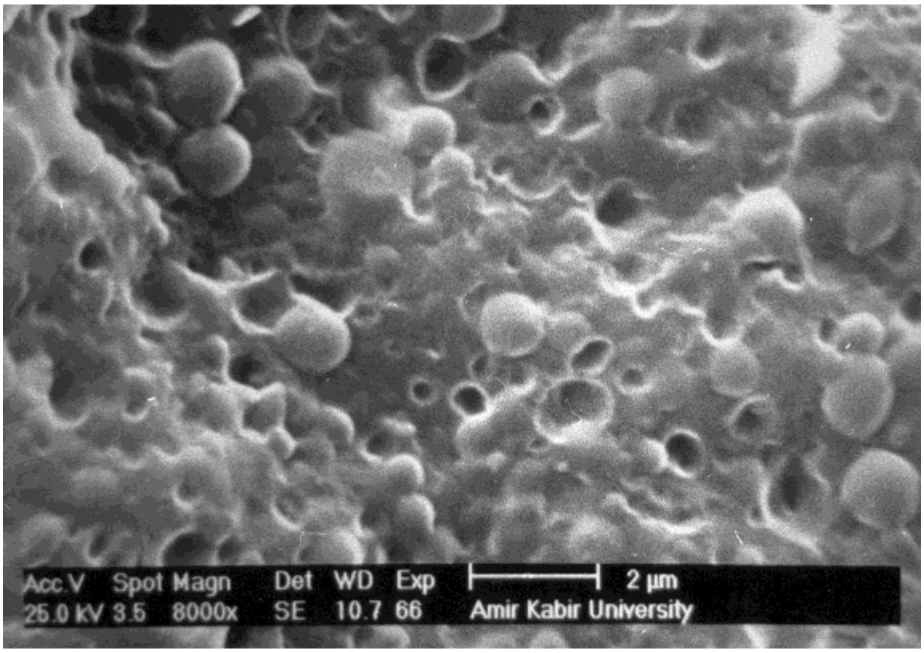

(B)

Figure 5 Comparison between the morphology of the dynamically cured EPDM/PP (60/40 w/w) blend samples removed from the mix: (A) at the torque maximum and (B) 2 min after the torque maximum.

the upper bound of the Halpin Tsai equation. However, for the uncured sample cooled at room temperature, the storage modulus was close to that predicted by the parallel model. Similar reports have also been published by Thomas and George[24] for ethylene vinyl acetate/polypropylene (EVA/PP) dynamically cured TPEs. These results suggest a partially cocontinuous morphology for

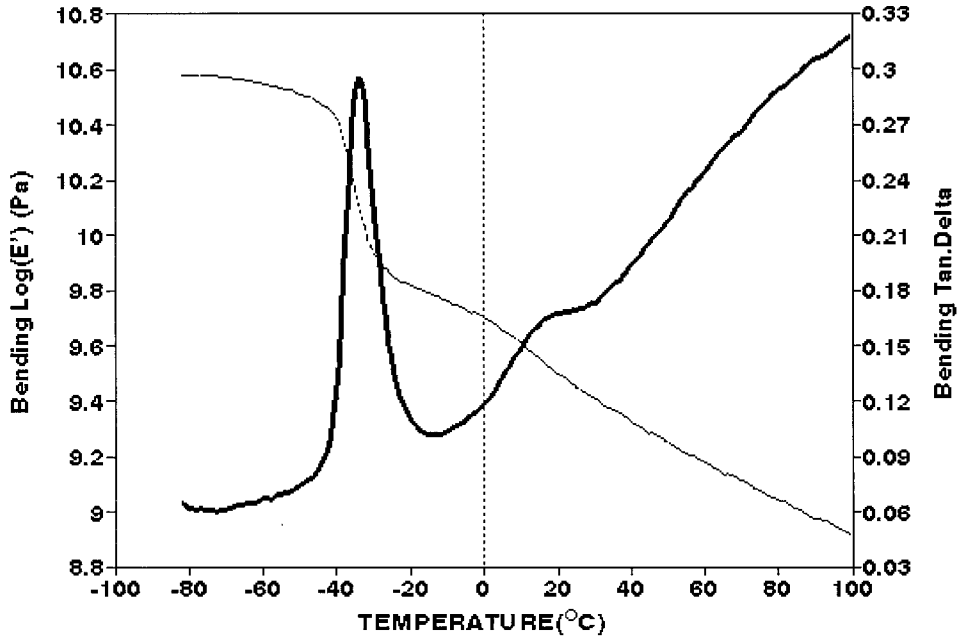

Figure 6 Variation of the storage modulus (· · ·) and loss tangent (—) with temperature for the uncured EPDM/PP (60/40 w/w) blend sample frozen immediately after removal from the hot running mix.

the uncured sample cooled at room temperature and a matrix-dispersed type of microstructure for both the dynamically cured and uncured but frozen samples, which is in agreement with the morphologies presented in Figures 3 and 4(B_4) for these blend samples.

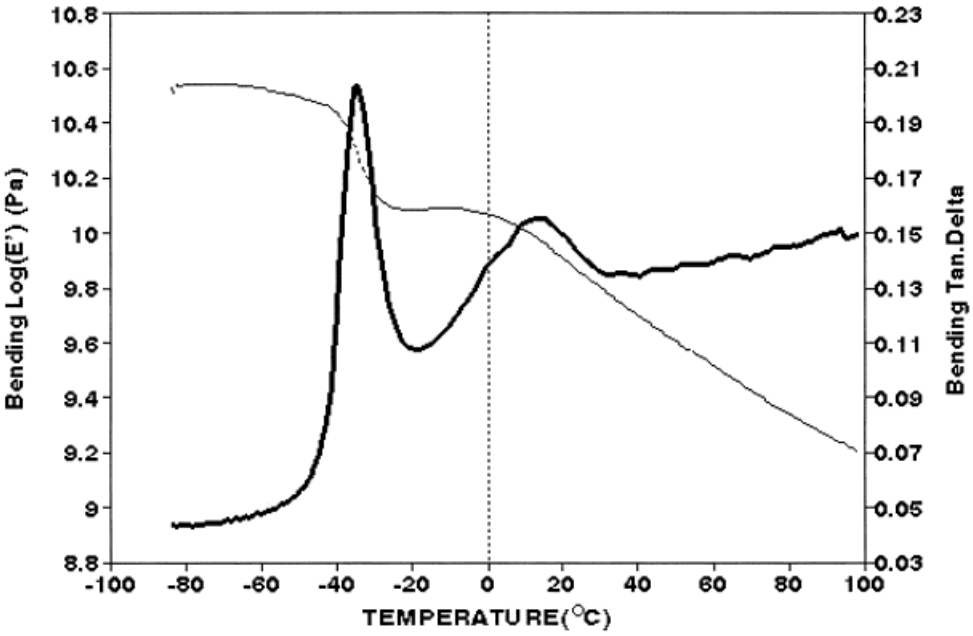

Figure 7 Variation of the storage modulus (· · ·) and loss tangent (—) with temperature for the uncured EPDM/PP (60/40 w/w) blend sample cooled at room temperature after removal from the hot running mix.

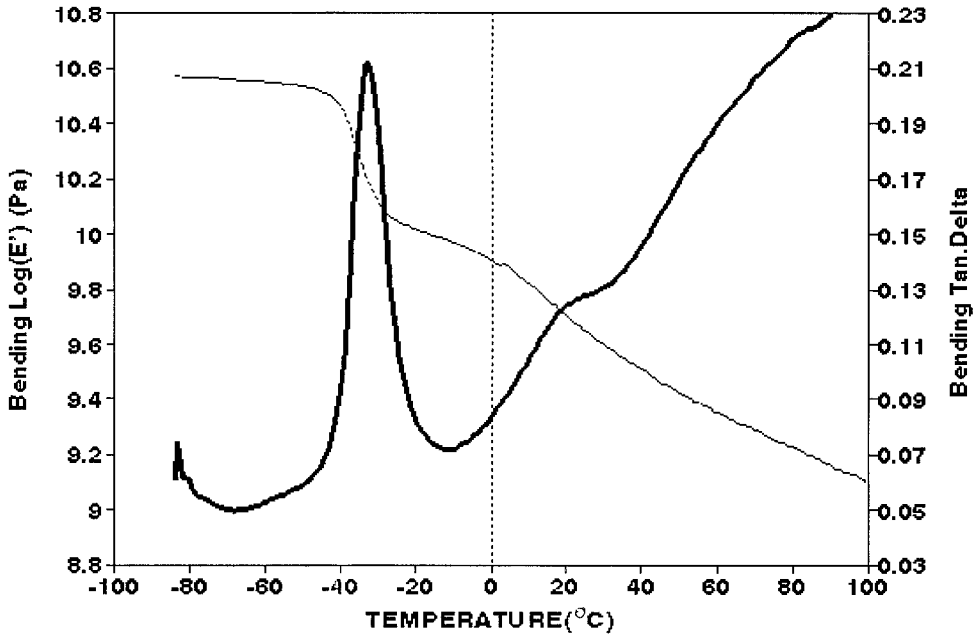

Figure 8 Storage modulus (· · ·) and loss tangent (—) versus temperature for the dynamically crosslinked EPDM/PP (60/40 w/w) blend sample removed from the hot running mix 2 min after attainment of the torque maximum.

From the obtained results, we are led to the conclusion that for the uncrosslinked thermoplastic rubber blends, the extent of the coalescence of the rubber droplets after being removed from the mixing process plays an important role in determining the final morphology of the blend. In other words, dynamic vulcanization can direct the microstructural development of the blend toward a matrix-dispersed type of morphology by preventing the coalescence of the rubber particles from the early stage of the dynamic vulcanization. Therefore, the mechanism of the microstructural development for the dynamically crosslinked TPEs can be modeled

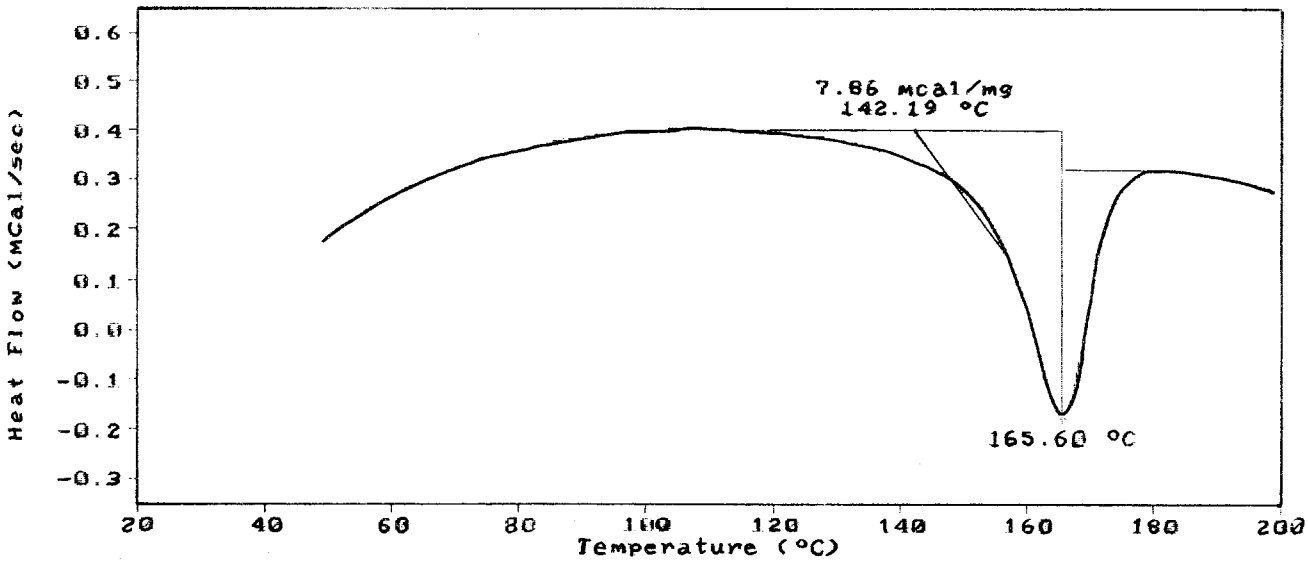

Figure 9 Differential scanning calorimetry thermogram of the uncured EPDM/PP (60/40 w/w) blend sample frozen immediately after removal from the hot running mix.

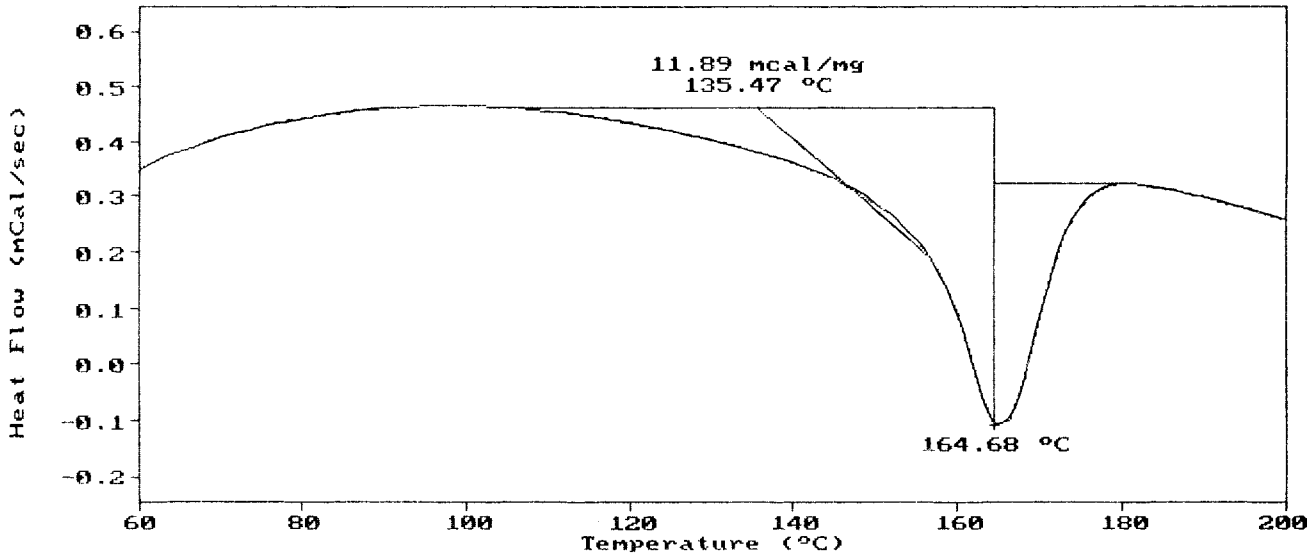

Figure 10 Differential scanning calorimetry thermogram of the uncured EPDM/PP (60/40 w/w) blend sample cooled at room temperature after removal from the hot running mix.

as schematically shown in Figure 13. This model consists of four stages:

1. The melt–melt dispersion, which is associated with the rubber-phase droplet breakup and coalescence before the onset of curing.
2. The occurrence of dynamic vulcanization through which the agglomeration of the cured rubber particles takes place, together with the droplet breakup process at a low SOC.
3. The increase in interfacial adhesion between the two phases as the vulcanization proceeds.
4. The breakdown of the agglomerates as a

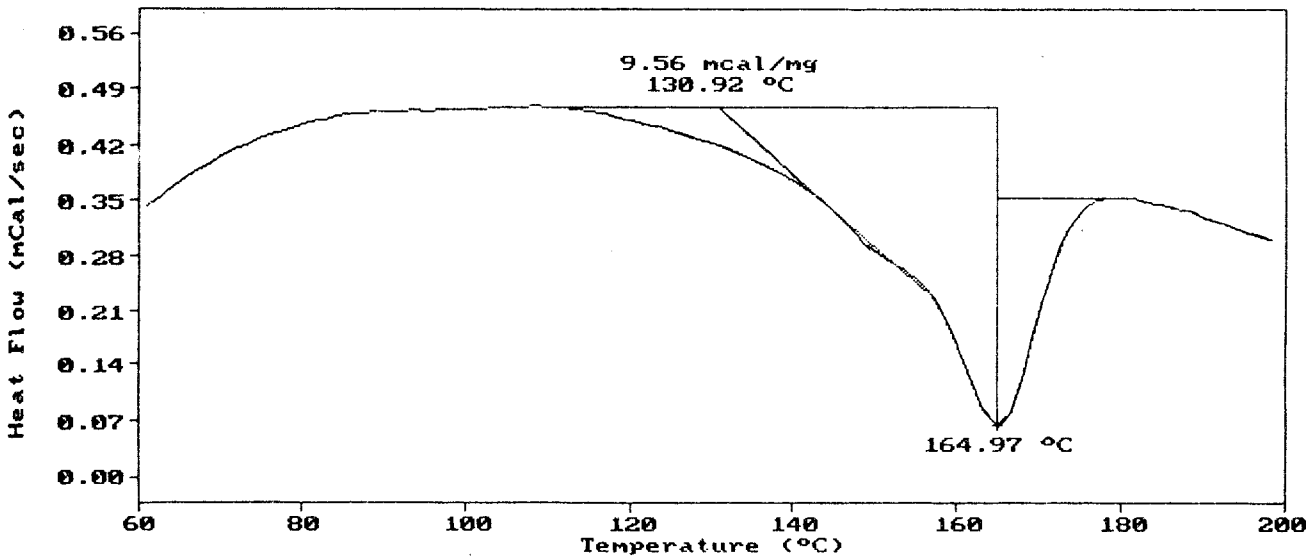

Figure 11 Differential scanning calorimetry thermogram of the dynamically cured EPDM/PP (60/40 w/w) blend sample removed from the hot running mix 2 min after attainment of the torque maximum.

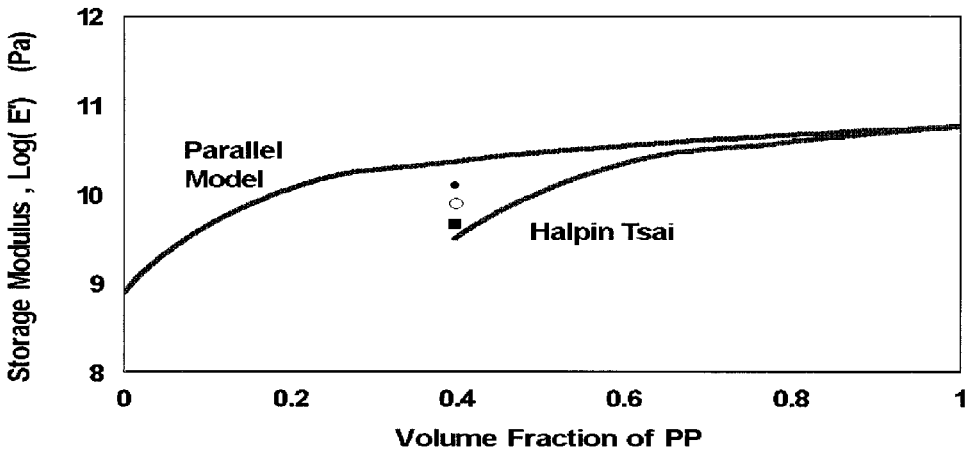

Figure 12 Effect of the volume fraction of EPDM on the storage modulus of EPDM/PP blends at 0°C: (●) uncured blend sample cooled at room temperature, (○) dynamically crosslinked blend sample, and (■) uncured blend sample frozen after removal from the mixer.

result of the applied shear forces and the shrinkage of the rubber particles at a higher degree of crosslinking to lower the surface energy. This finally leads to the more uniform dispersion of the rubber particles throughout the thermoplastic matrix.

CONCLUSIONS

The morphology of the EPDM/PP (60/40 w/w) blends in the melt–melt mixing stage was a matrix-dispersed type consisting of rubber particles dispersed throughout the PP matrix, which was simultaneously controlled by the rate of breakup

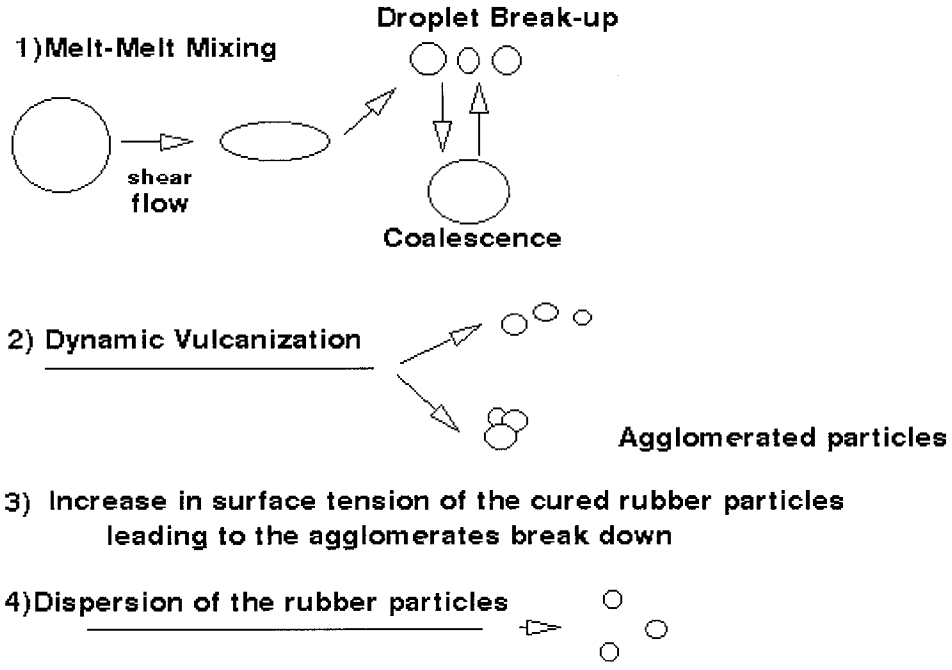

Figure 13 Schematic diagram of the proposed model to describe the mechanism of morphological dynamically cured TPE.

and the coalescence of the rubber droplets as two mutual mechanisms. However, when the molten samples of these blends were cooled at room temperature, a particulate cocontinuous two-phase morphology was observed as the coalescence of the rubber particles predominated.

The dynamic vulcanization process can play a significant role in enhancing the interfacial interaction between the two phases, leading to the formation of a stabilized and well-defined matrix-dispersed type of morphology.

From our results, a model consisting of four stages describing the development of the morphology for dynamically cured EPDM/PP (60/40 w/w) TPEs is proposed.

The authors kindly thank the Iran Polymer Research Center for its experimental assistance.

REFERENCES

1. Fisher, W. K. U.S. Pat. 3,758,643, 1973.
2. Fisher, W. K. U.S. Pat. 3,862,106, 1975.
3. Coettler, L. A.; Richwine, J. R.; Wille, F. J. Rubber Chem Technol 1982, 55, 1448.
4. Coran, A. Y.; Patel, R. Rubber Chem Technol 1981, 54, 892.
5. Morris, H. L. In Handbook of Thermoplastic Elastomers; Walker, B. M., Ed.; Van Nostrand Reinhold: New York, 1979; Chapter 2.
6. Moffett, A. J.; Dekkers, M. E. J. J Polym Eng Sci 1992, 32.
7. Abdou-Sabet, S.; Patel, R. P. Rubber Chem Technol 1991, 64, 769.
8. Ghosh, P.; Chattopadhyay, B.; Sen, A. K. Polymer 1994, 35, 18.
9. Danesi, S.; Porter, R. S. J Polym 1978, 19, 448.
10. Kresge, E. N. Rubber Chem Technol 1991, 64, 469.
11. Abdou-Sabet, S.; Puydak, R. C.; Patel, R. P. Rubber Chem Technol 1996, 69, 479.
12. Kresge, E. N. In Polymer Blends; Paut, D. R.; Newman, S., Eds.; Academic: New York, 1978; Chapter 20, p 2.
13. Kuriakose, B.; De, S. K. J Appl Polym Sci 1986, 32, 5509.
14. Laokucharoen, P.; Coran, A. Y. Rubber Chem Technol 1998, 71, 966.
15. Bhowmick, A. K.; Inoue, T. J Appl Polym Sci 1993, 49, 1983.
16. Wu, S. Polymer Interface and Adhesion; Marcel Dekker: New York, 1982.
17. Nielsen, L. E.; Landel, R. E. Mechanical Properties of Polymers and Composites, 2nd ed.; Marcel Dekker: New York, 1994.
18. Wu, S. In Polymer Blends; Paul, D. R.; Newman, S., Eds.; Academic: New York, 1978; Vol. 1, p 243.
19. Wu, S. J Macromol Sci C 1974, 10, 1.
20. Chung, O.; Coran, A. Y. Rubber Chem Technol 1998, 70, 781.
21. Garbassi, F. Polymer Surfaces; Wiley: Chichester, England, 1995; Chapter 1.
22. Nielsen, N. E. Rheol Acta 1974, 13, 86.
23. Halpin, J. C. J Compos Mater 1970, 3, 732.
24. Thomas, S.; George, A. Eur Polym J 1995, 28, 1451.